ELSEVIER

Biochimica et Biophysica Acta 1370 (1998) 77–86

BIOCHIMICA ET BIOPHYSICA ACTA
BBA

Topological study of *Vibrio alginolyticus* NhaB Na^+/H^+ antiporter using gene fusions in *Escherichia coli* cells

Hiromi Enomoto [a], Tsutomu Unemoto [a], Mitsuaki Nishibuchi [b], Etana Padan [c], Tatsunosuke Nakamura [a,*]

[a] *Laboratory of Membrane Biochemistry, Faculty of Pharmaceutical Sciences, Chiba University, 1-33 Yayoi-cho, Inage-ku, Chiba 263, Japan*

[b] *Division of Human Environment, Center for Southeast Asian Studies, Kyoto University, 46 Shimoadachi-cho, Yoshida, Sakyo-ku, Kyoto 606-01, Japan*

[c] *Division of Microbial and Molecular Ecology, the Institute of Life Sciences, the Hebrew University of Jerusalem, 91904 Jerusalem, Israel*

Received 4 August 1997; revised 22 September 1997; accepted 3 October 1997

Abstract

NhaB, an Na^+/H^+ antiporter, of *Vibrio alginolyticus* is a 528-amino-acid protein. Hydropathy profile-based computer analysis predicted that the NhaB might contain up to 13 membrane-spanning domains. To examine this hypothesis, we applied the *phoA* fusion method to the cloned *nhaB* gene. Eighteen plasmid-borne *nhaB–phoA* fusion genes were constructed in *Escherichia coli* cells and the alkaline phosphatase activity and expression level of the fusion proteins analyzed. These results and the results obtained with additional constructs indicated that *V. alginolyticus* NhaB has a unique topology consisting of nine transmembrane segments with the N-terminus in the cytoplasm and the C-terminus in the periplasm. © 1998 Elsevier Science B.V.

Keywords: Sodium ion/proton antiporter; *nhaB* gene; Topology; Marine bacterium; (*Vibrio alginolyticus*)

1. Introduction

The Na^+/H^+ antiporters extrude Na^+ in exchange for external H^+ in bacteria [1]. The antiporters have been thoroughly studied in *Escherichia coli*. This bacterium contains three antiporter genes, *nhaA* [2], *nhaB* [3] and *chaA* [4]. *E. coli* TO114, in which the three genes were deleted, became highly sensitive to external Na^+ [5]. The *nhaA* gene of *Salmonella entiritidis* and the *nhaAB* genes of *Vibrio alginolyticus* and *V. parahaemolyticus* were cloned by functional complementation of Na^+/H^+ antiporter-defective *E. coli* strains [6–10]. The *nhaAB* homolog was found in *Haemophilus influenzae* by homology search of the whole genome sequence [11].

The two-dimensional model of NhaA has recently been proposed [12,13]. We demonstrated by site-directed mutagenesis that the conserved negatively charged aspartic acid residues in the proposed trans-

* Corresponding author. Fax: +81-43-2903021; E-mail: tnakha@p.chiba-u.ac.jp

PII S0005-2736(97)00245-9

membrane segments (TMs) of NhaA of *V. alginolyticus* (Va–NhaA) are important for Na^+/H^+ antiport activity [14]. The importance of the conserved aspartic acid residues in NhaA of *E. coli* was also suggested indirectly by a fluorescent technique [15].

NhaB differs considerably from the NhaA family of antiporters; its H^+/Na^+ stoichiometry is 3/2 [16] as opposed to 2/1 for NhaA [17]; Like the eukaryotic Na^+/H^+ antiporters, NhaB but not NhaA is sensitive to amiloride [18]; there is very little amino acid sequence homology between NhaA and NhaB. Nevertheless, both proteins function as Na^+/H^+ antiporters. Therefore, it would be interesting to study NhaB for its secondary structure and the essential residues. Pinner et al. [3] suggested that NhaB of *E. coli* has 12 TMs. This was simply based on the hydropathy profile predicted by the standard method [19].

Alkaline phosphatase (PhoA) of *E. coli* is enzymatically active only when it is exported across the inner membrane into the periplasm. Therefore, a high level of PhoA activity exhibited by a PhoA fusion protein in *E. coli* indicates that the fusion joint is located on the periplasmic side of the membrane. The PhoA gene (*phoA*) fusion method that was originally developed by Beckwith et al. [20–22] has thus been applied to the topological study of many membrane proteins [12,23–28]. For example, Geller et al. [27] studied the topology of the eukaryotic membrane protein Ste6 by *phoA* fusion in *E. coli* and by invertase fusion in yeast and concluded that *phoA* gene fusion in *E. coli* is applicable to topological study of foreign membrane proteins expressed in *E. coli*. We chose this approach to determine the topological model of NhaB cloned from the marine bacterium, *V. alginolyticus* (Va–NhaB).

2. Materials and methods

2.1. Bacterial strains and growth conditions

E. coli DH5α [29] was used as a host for site-directed mutagenesis and plasmid preparation. *E. coli* strains CC118 [21] and UT5600 (*ara14*, *leuB6*, *azi6*, *lacY1*, *proC14*, *tsx67*, *supE44*, Δ[*ompT–fepC*]266, *entA403*, λ⁻, *trpE38*, *rfbD1*, *rpsL109*, *xyl5*, *mtl1*, *thi1*, obtained from the *E. coli* Genetic Center at Yale University) were used as hosts for PhoA activity determinations. *E. coli* TO114 (Δ*nhaA*, Δ*nhaB*, Δ*chaA*) grows in LBK100 medium (1% polypeptone, 0.5% yeast extract, 100 mM KCl, pH 7.0) but not in LBK100Na200 medium (LBK100 with 200 mM NaCl) [5].

2.2. Gene fusions

To construct Va–NhaB–PhoA fusion proteins, pPAB404 containing the *Kpn*I–*Pst*I cloning sites for *phoA* fusion [24] was employed as the fusion vector. A recombinant plasmid, pTN1, contains the complete *nhaB* gene cloned from *Vibrio alginolyticus* [9]. This plasmid served as the template for the polymerase chain reaction amplification to obtain the *Kpn*I–*Pst*I DNA fragments encoding partial NhaB polypeptides (from N-terminal to the fusion joints). The primers used for the amplification are listed in Table 1. The primer designated NhaB/*Kpn*I annealed to the sequence 166 bp upstream of the start of the *nhaB* coding sequence and contained the *Kpn*I-specific sequence. The other primers served as distal in-frame *Pst*I site primers for selected fusion joints. The amplified fragments were purified, digested with *Kpn*I

Table 1
Oligonucleotide primers used for construction of the KpnI–PstI DNA fragments carrying partial *nhaB* sequences

NhaB/*Kpn*I	ATGGTACCGAGCGGTGCTTGAGTTCAGGGG
*Pst*I/P41	ATCTGCAGTGGGTTTATTAGGAAGAATACA
*Pst*I/E51	ATCTGCAGTTCAGCAACCAGCAACCACCCA
*Pst*I/K61	ATCTGCAGTTTTAATGCCATTGCAAGCGTG
*Pst*I/E89	ATCTGCAGCTCGTGCTTAACTTGCGCAGGG
*Pst*I/K128	ATCTGCAGTTTGGAGCGAATACCAAGTAAA
*Pst*I/R202	ATCTGCAGGCGTAAAAAGGCGCGGTAATTT
*Pst*I/E239	ATCTGCAGTTCACCAAATAACCAACCCGCT
*Pst*I/K300	ATCTGCAGTTTTGCAACGTCTTGATTGGTA
*Pst*I/E351	ATCTGCAGCTCTTCAAACGCTTTACCCATG
*Pst*I/E386	ATCTGCAGTTCAACGGCAAGCACCGCGTCG
*Pst*I/D434	ATCTGCAGGTCGAACTGCTCGCGAGTAATG
*Pst*I/R476	ATCTGCAGTCTACCGTAAGACAGACGAATT
*Pst*I/D519	ATCTGCAGATCACCACTATGAGGTAAAATC
*Pst*I/E74	ATCTGCAGTTCAATAGCAAGTAAACCACCA
*Pst*I/E95	ATCTGCAGCTCAATATTTGCCACCAACTCG
*Pst*I/D147	ATCTGCAGATCCAAAAACGCAGATAAAAATG
*Pst*I/A320	ATCTGCAGCGCCAAGTGTAAGGCTAATGCT
*Pst*I/P452	ATCTGCAGTGGCGTAGCAACAGATGGTAGG

and *Pst*I, and then cloned into the *Kpn*I–*Pst*I sites of pPAB404. The resulting plasmids were designated pBXxxx, where X is the one-letter symbol of the amino acid residue at the fusion joint and xxx is the residue number. All *phoA* fusion joints in pBXxxx plasmids were confirmed by sequencing through the fusion joints in the backward direction, using a primer 5′-ACCTTCGGCATAATTACGTGCGGC-3′, which is complementary to the *phoA* gene sequence (145 bp down stream of the fusion joint). Va–NhaB–PhoA fusion proteins encoded in pBXxxx plasmids are indicated as XxxxPhoA proteins.

The *nhaB* gene of *V. alginolyticus* (*Va–nhaB*) has two *Mlu*I sites within the coding sequence: pBK300, one of the pBXxxx plasmids constructed as above, retained the two *Mlu*I sites and had another *Mlu*I site in the vector sequence. pBK300 was partially digested with *Mlu*I and religated. One of the resulting plasmids that lost the 306 bp *Mlu*I fragment internal to the *nhaB* gene was obtained. This plasmid and the fusion protein encoded by the plasmid were named pBK300ΔM and K300ΔMPhoA, respectively. The *Mlu*I junction of pBK300ΔM was confirmed by DNA sequencing.

2.3. PhoA activity

PhoA activity of CC118 or UT5600 cells harboring *Va–nhaB–phoA* fusion plasmids (pBXxxx and pBK300ΔM) was roughly estimated by blue coloration of the colonies on LB agar plates containing 5-bromo-4-chloro-3-indolyl-phosphate (toluidine salt; XP) at a concentration of 40 μg/ml. The exact activity level was determined by measuring the rate of *p*-nitrophenol phosphate hydrolysis [20]. Briefly, the test strain was grown in LB medium containing ampicillin until the optical density at 600 nm reached 0.2. Isopropyl-1-thio-β-D-galactopyranoside was added to achieve the final concentration of 1 mM and the culture was incubated for another 2 h by shaking at 37°C. Thereafter, cells were harvested from 1.4 ml culture and suspended in 1 ml of 10 mM Tris-0.1 M NaCl buffer (pH 8.0). A 0.1 ml aliquot was transferred into a new tube and 0.9 ml of 1 M Tris-HCl (pH 8.0) added. Cells were lysed by addition of 50 μl each of 0.1% SDS and chloroform, and reactions were started by addition of 100 μl of 0.4% *p*-nitrophenyl phosphate and incubated at 37°C. To stop the reaction, 0.1 ml of 1 M KH_2PO_4 was added. The absorbances of the reaction mixtures were then read at 420 nm and 550 nm. PhoA unit was calculated as described by Brickman and Beckwith [20].

2.4. Immunoblot analysis

The bacterial cells prepared for the PhoA assay as described in the foregoing (suspended in 10 mM Tris-HCl, 0.1 M NaCl buffer [pH 8.0]) were lysed and total proteins solubilized by treatment with 2 × SDS loading buffer [30].

Protein concentration was determined by the method of Lowry et al. [31], with bovine serum albumin as the standard. A total of 20 μg proteins were separated by electrophoresis on 12% SDS-polyacrylamide gels and transferred electrophoretically to PVDF membranes (Bio-Rad). Immunoblot detection was performed as described by Allard and Bertrand [32]. Polyclonal rabbit anti-*E. coli* alkaline phosphatase antibody (Rockland, Gilbertsville, PA) and anti-rabbit IgG/alkaline phosphatase-labeled pig antibody (DAKO, Denmark) were used for detection of the PhoA fusion proteins.

2.5. Computer analysis

Hydropathic profile of the deduced amino acid sequence of the Va–NhaB was predicted by the computer-assisted procedure according to the methods of Kyte and Doolittle [33]. The possible TMs of the Va–NhaB sequence was deduced by a computer program TopPredII [34].

3. Results and discussion

3.1. Construction of Va–nhaB–phoA fusion

The hydropathy profile and the putative TMs sequence were predicted from the Va–NhaB by the standard computer-assisted methods (Fig. 1(A)). To determine the topology of the Va–NhaB, a series of 18 Va–NhaB–PhoA fusions were constructed by gene

fusion. In these constructs, PhoA was fused to the residue in, or adjacent to the presumed loops located between the predicted TMs (indicated by the arrows in Fig. 1(A)). The fusion joints are also shown in the deduced amino acid sequence of Va–NhaB (Fig. 1(B)).

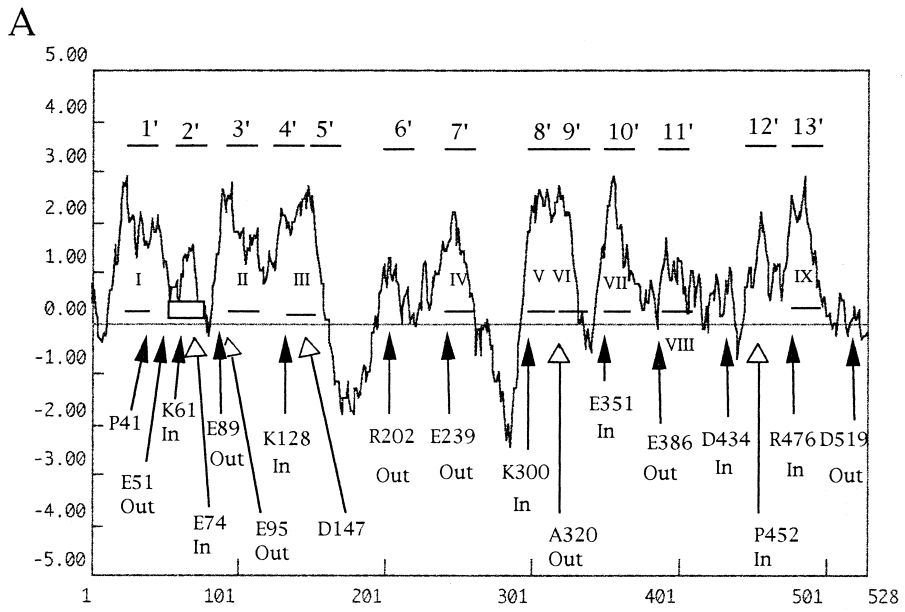

B

1" MPISLGNAFIKNFLGKAPDWYKVAIIAFLIINPIVFFLINPFVAGWLLVAEFIFTLAMAL 60"
61" KCYPLQPGGLLAIEAIAIGMTSPAQVKHELVANIEVLLLLVFMVAGIYFMKHLLLFIFTK 120"
121" ILLGIRSKTLLSLAFCFAAAFLSAFLDALTVIAVVISVAIGFYSIYHKVASGNPIGDHDH 180"
181" TQDDTITELTRDDLENYRAFLRSLLMHAGVGTALGGVTTMVGEPQNLIIADQAGWLFGEF 240"
241" LIRMSPVTLPVFFCGLITCALVEKLKVFGYGAKLPNNVRQILVDFDNEERKTRTNQDVAK 300"
301" LWVQGLIAVWLIVALALHLAAVGLIGLSVIILATAFTGVIEEHSMGKAFEEALPFTALLA 360"
361" VFFSIVAVIIDQELFKPVIDAVLAVEDKGTQLALFYVANGLLSMVSDNVFVGTVYINEVK 420"
421" TALIEGLITREQFDLLAVAINTGTNLPSVATPNGQAAFLFLLTSALAPLIRLSYGRMVIM 480"
481" ALPYTIVLAIVGLMGIMFFLEPATASFYDAGWILPHSGDLTPVVSGGH 528"

I 41 51
2' 3'
61 74 89 95 II
4' 5'
128 III 147
6'
202 239
7'
IV 300
8' 9' 10'
V 320 VI 351 VII
11'
386 VIII
12'
434 452 476
13'
IX 519

Table 2
Properties of NhaB–PhoA fusion proteins

Designation [a]	Colony color on XP plate	PhoA activity (units) in		Number of residues / MW (Da)
		CC118	UT5600	
P41PhoA	B [b]	710	710	481/50690
E51PhoA	B [b]	1200	920	491/51777
K61PhoA	W [b]	4	1	501/52913
E74PhoA	W [b]	ND [c]	10	514/54262
E89PhoA	B [b]	33	69	529/55804
E95PhoA	B [b]	ND [c]	1100	535/56439
K128PhoA	W [b]	0	2	587/62280
D147PhoA	B [b]	ND [c]	293	587/62280
R202PhoA	B [b]	237	58	642/68395
E239PhoA	B [b]	80	106	679/72132
K300PhoA	W [b]	26	4	740/79072
A320PhoA	B [b]	ND [c]	164	760/81253
E351PhoA	W [b]	15	3	791/84439
E386PhoA	B [b]	1334	144	826/88195
D434PhoA	W [b]	8	5	874/93470
P452PhoA	W [b]	ND [c]	1	892/95204
R476PhoA	W [b]	6	3	916/97779
D519PhoA	B [b]	803	249	959/102434
None (pPAB404)	W [b]	0	1	NA [d]
K300ΔMPhoA	B [b]	233	ND	638/67740

[a] See text.
[b] B, blue; W, white.
[c] ND, not determined.
[d] NA, not applicable.

3.2. PhoA activities and expressions of Va–NhaB–PhoA fusion proteins

pBXxxx Plasmids encoding 13 different Va–NhaB–PhoA fusion proteins (filled arrow-heads in Fig. 1(A), filled triangles in Fig. 1(B)) were first transformed into CC118, a commonly employed host for PhoA assay. The colors of the colonies on XP plates and the levels of the PhoA activities are summarized in Table 2. The strains having 33 units or higher of PhoA activity formed blue colonies. The expressions of the 13 fusion proteins in CC118 were confirmed by the immunoblot analysis with anti-PhoA antibody (Fig. 2(A)). The antibody-positive bands were detected at the positions corresponding essentially to the predicted molecular weights of the fusion proteins (Table 2). The reason for the appearance of additional bands of higher molecular weights in

Fig. 1. Hydropathy plot and (A) the deduced TMs of NhaB of *V. alginolyticus* (Va–NhaB) and (B) the deduced amino acid sequence. The average hydrophobicity calculated by the method of Kyte and Doolittle [33] is plotted on the vertical axis vs. the residue number on the horizontal axis. Higher values represent greater hydrophobicity. The 13 TMs predicted by TopPredII program [34] are indicated by the lines with Arabic numerals with primes (A and B). The nine TMs proposed by PhoA fusion analysis in this study are depicted by the lines with Roman numerals (A and B) (see Fig. 3 below). A predicted hairpin region between TMI and TMII is denoted by (A) □ or (B) · · · . The positions of the joints selected for PhoA fusion are indicated by the arrows (A). The amino acid residues in one-letter symbols and the residue numbers of the joints are described. The filled and open arrowheads indicate that the PhoA activity of the fusion protein was measured, respectively, in both CC118 and UT5600 backgrounds or only in a UT5600 background (see Table 2). The phoA gene fusion joints are denoted below the Va–NhaB sequence by triangles with the corresponding residue numbers. The filled and open triangles of (B) correspond to the filled and open arrowheads of (A), respectively.

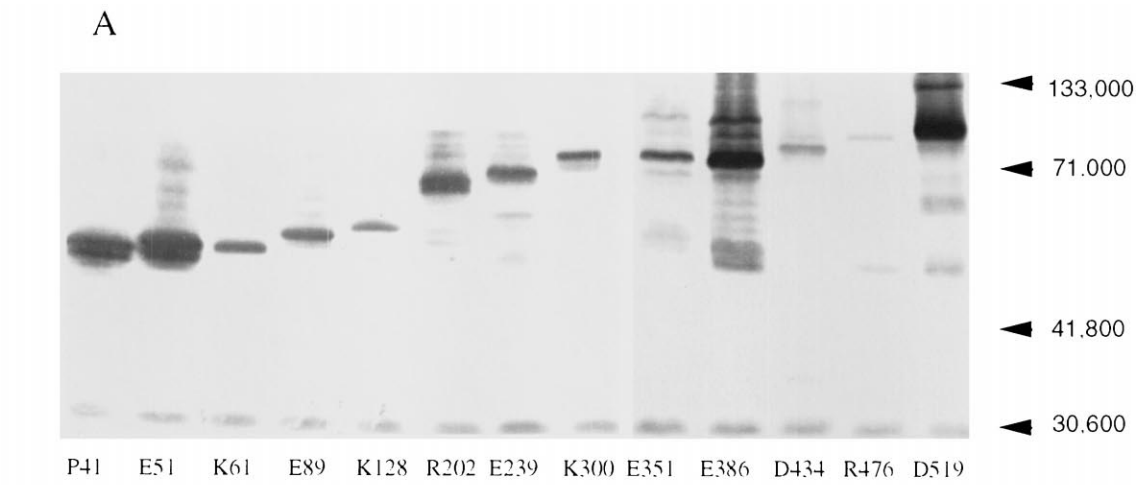
A
133,000
71,000
41,800
30,600
P41 E51 K61 E89 K128 R202 E239 K300 E351 E386 D434 R476 D519

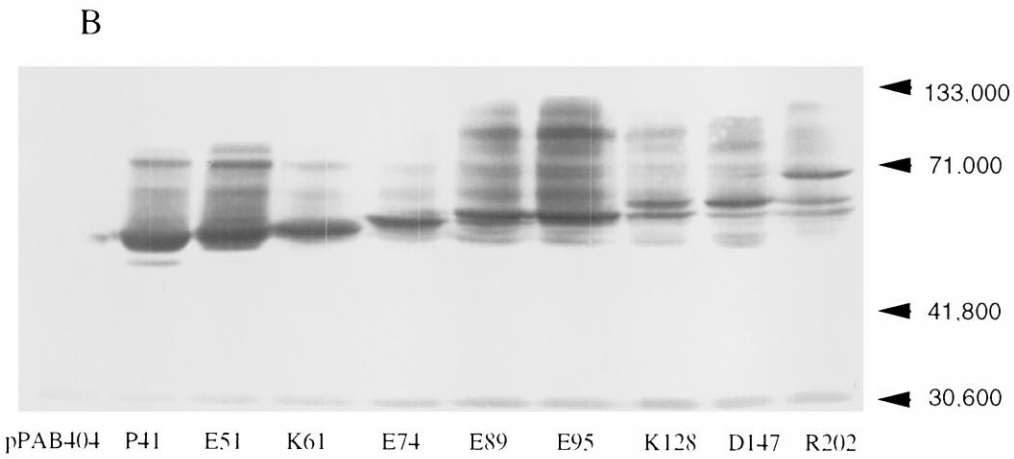
B
133,000
71,000
41,800
30,600
pPAB404 P41 E51 K61 E74 E89 E95 K128 D147 R202

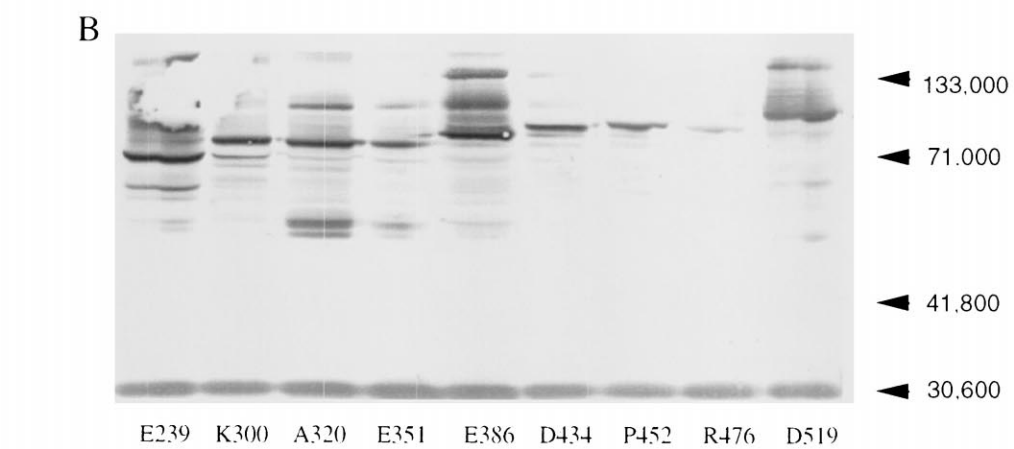
B
133,000
71,000
41,800
30,600
E239 K300 A320 E351 E386 D434 P452 R476 D519

E51PhoA, R202PhoA, E239PhoA, E351PhoA, E386PhoA, D434PhoA and D519PhoA is unknown, but bands of lower molecular weights may be degradation products of the fusion proteins. The expressions of P41PhoA, E51PhoA, R202PhoA, E386PhoA and D519PhoA were higher than the other fusion proteins.

The results shown in Table 2 suggest that the fusion joints P41, E51, R202, E386, and D519 are in or near the periplasmic side of the respective TMs. Cells producing E89PhoA and E239PhoA formed blue colonies on XP plates and exhibited relatively low but significant PhoA activities (Table 2), suggesting the possibility that junctions E89 and E239 are also located in the periplasm. Cells carrying K61PhoA, K128PhoA, E351PhoA, D434PhoA and R476PhoA formed white colonies and exhibited very low levels or no PhoA activity, suggesting that the fusion junctions of these proteins are at or near the cytoplasmic side of the respective TMs.

CC118 cells producing K300PhoA formed white colonies but exhibited significant PhoA activity. Therefore, all the above fusion proteins were reexamined in the *E. coli*, UT5600 background. UT5600 has been shown to be useful for topological experiments [23]. The results are listed in Table 2. The colors of the colonies were the same as those observed with the CC118 background. The UT5600 transformants producing active fusion proteins were similar to those of CC118. However, the UT5600 transformants producing white colonies exhibited lower levels of PhoA activity than the corresponding CC118 derivatives. Five new fusion proteins (E74PhoA, E95PhoA, D147PhoA, A320PhoA and P452PhoA [Fig. 1A – open arrow-heads; Fig. 1B – open triangles]) were also examined in the UT5600 background (Table 2). The results indicate that the E95, D147 and A320 joints appear to be located at the periplasmic side while that of both E74PhoA and P452PhoA at the cytoplasmic side. In all cases, the fusion proteins were expressed in UT5600 cells (Fig. 2(B)). Although expression of R476PhoA was low, it was still detectable. Accordingly, we concluded that the blue and white colony colors can be used to predict, respectively, the periplasmic and cytoplasmic location of the fusion joint.

3.3. Membrane topology model

We predicted the membrane topology model of Va–NhaB, as illustrated in Fig. 3, by combining the hydropathy and TM data of the computer analysis and the results of PhoA fusion analysis and additional analyses described below. The N-terminus with net positive charge of many membrane proteins is usually located in the cytoplasm [35]. The N-terminus of Va–NhaB has three positively charged amino acids (K11, K16 and K22) and one acidic amino acid (D19).

The PhoA fusion results indicated that P41, E51, E89 and E95 are located in the periplasm and K61 and E74 in the cytoplasm. It is likely that the first TM (TMI, Fig. 3) extends from V23 to V43 (hereafter abbreviated as V23/V43) as predicted by the hydropathy profile and TopPredII analysis (Fig. 1). Although there is plenty of room for two normal transmembrane segments between residues 43 and 96, the hydropathy profile (Fig. 1(A)) indicates a single weak hydrophobic region. Since K61 and E74 are not located in the periplasic side (Table 2), we consider that there may be a hairpin sequence located inside the membrane (Fig. 3), which is similar to those described as the H5 and P loops in ion channels and bacterial K^+ transport systems [36,37]. Further experiments are needed to support this hypothesis.

Since E95 is periplasmic and K128 is cytoplasmic, it is predicted that TMII is V96/L115. Thus, four TMs were predicted between K128 to K300, according to the hydropathy-based TopPredII program (4′–7′, Fig. 1(A)). Both R202 and K300 are predicted to be on the cytoplasmic side, while E239 on the periplasmic side in this model. However, the PhoA fusion results (Table 2) do not agree with this model. The results suggest instead that both, R202 and E239

Fig. 2. Immunoblot analysis for Va–NhaB–PhoA fusion proteins expressed in *E. coli* (A) CC118 or (B) UT5600. Samples were separated by electrophoresis and western blotting was performed. The fusion proteins reacting with an anti-*E. coli* PhoA antibody were stained. Designation for the fusion joint (amino acid residue in one-letter symbol and residue number, Fig. 1) is used to indicate each fusion protein.

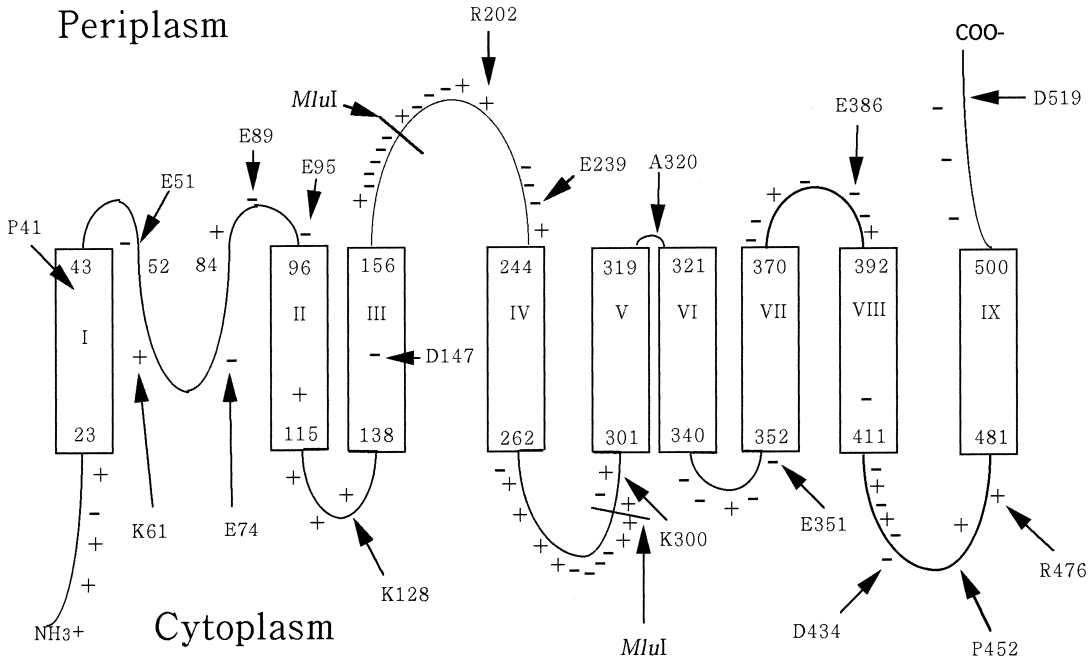

Fig. 3. Membrane topology of Va–NhaB proposed by PhoA fusion analysis. Transmembrane segments (I–IX) are shown as open squares. Charged amino acids are indicated by + (Arg and Lys) and − (Asp and Glu). The borders of TMs are generally based on those predicted by the TopPredII program [26]. The 18 *phoA* gene fusion joints are designated by arrows. See the legend of Fig. 1 and text for the designations. The *Mlu*I restriction sites are also indicated.

are in the periplasm and that only one TM (TMIII, Fig. 3) exists between K128 and R202. There is a long hydrophobic region between T129 and G172 (Fig. 1(A)). We consider that TMIII is located in the middle of this region, A138/I156. This predicted TMIII region is highly hydrophobic with a single acidic amino acid, D147.

Two more hydrophobic regions were predicted between R191 to K300 (6′ and 7′, Fig. 1(A)). To determine the number of TM(s) between R191 and T292, we constructed a fusion protein K300ΔMPhoA, in which the PhoA fusion site is at K300 but a peptide from R191 to T292 is deleted by deletion of the *Mlu*I fragment from pBK300. CC118 cells, producing K300ΔMPhoA formed blue colonies on XP plates and had high-level of PhoA activity (Table 2). K300ΔMPhoA detected by the immunoblotting (Fig. 4) showed the migration distance corresponding to the predicted molecular weight (68 kDa). The result shows that the deletion converted the location of K300 from the cytoplasmic to the periplasmic side. Hence, there should be only one TM in this region. E239 is located in the periplasmic region (Table 2), so that TMIV appears to be located in M244/V262 (Fig. 3). The result that the TMIV region is more hydrophobic than S203/E223 region (Fig. 1(A)) supports this TMIV assignment.

K300 and E351 are on the cytoplasmic side and A320 is on the periplasmic side (Table 2), which led us to assign TMV to L301/L319 and TMVI to A321/I340 (Figs. 1 and 3). Similarly, the predicted locations of K351 and D434 (cytoplasmic) and E386 (periplasmic) allow us to assign TMVII to A352/I370 and TMVIII to L392/V411 (Fig. 3). Since P452 is cytoplasmic and D519 is periplasmic (Table 2), one TM probably exists between these residues. R476 was judged to be on the cytoplasmic side (Table 2). The A481/L500 region is more hydrophobic than N453/S473 (Fig. 1(A)), so that we assigned TMIX to A481/L500. Accordingly, the C-terminal was assigned to the periplasm.

Our proposed topological model for Va–NhaB (Fig. 3) fits well with the so-called ‘positive inside rule’ [38], except that our model contains negative

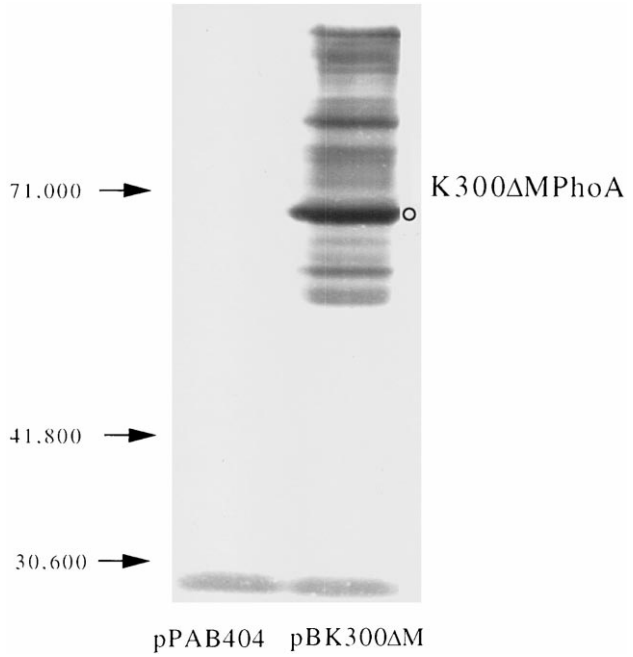

Fig. 4. Expressions of K300ΔMPhoA in CC118(pBK300ΔM). Samples were treated as in Fig. 2. Immunoblot analyses were done with an antibody for PhoA. The control strains carrying the fusion vectors, pPAB404, were compared with the test strains side-by-side. The major antibody-positive band is indicated by a circle.

loop region between TMVI and TMVII. In addition, our model is somewhat similar to the topological model suggested for CitS (a citrate carrier) in that the protein contains nine TMs and that the N-terminus is in the cytoplasm and the C-terminus in the periplasm [28].

V. alginolyticus has at least two Na^+/H^+ antiporters, Va–NhaA [7] and Va–NhaB [9]. We predicted that Va–NhaA has 12 TMs and that the N- and C-termini are in the periplasm [14]. Hence, the topological model of Va–NhaB that we proposed in this study is quite different from that of Va–NhaA. We showed that Va–NhaB has odd-numbered TMs, a property which is unusual for other transport proteins. Another unique property of our Va–NhaB topological model is a putative hairpin region. Further topological studies, such as cystein scanning mutagenesis [39], are needed for more complete determinations of the membrane spanning domains to support our prediction.

Acknowledgements

We greatly appreciate the kind gift of plasmid pPAB404 from Wolfgang Epstein that was constructed by Ki-Tae Kim (University of Chicago). We are also grateful to Dale A. Webster (Illinois Institute of Technology) for the continued encouragement and critical reading of the manuscript. This work was supported in part by a grant-in-aid for scientific research from the Japanese Ministry of Education, Science and Culture.

References

[1] E. Padan, S. Schuldiner, Bacterial Na+/H+ antiporters, in W.N. Konings, H.R. Kaback, J.S. Lolkema (Eds.), Handbook of Biological Physics, Vol. 2., Elsevier Science B.V., Amsterdam, 1996, pp. 501-531.

[2] R. Karpel, Y. Olami, D. Taglicht, S. Schuldiner, E. Padan, Sequencing of the gene *ant* which affects the Na^+/H^+ antiporter activity in *Escherichia coli*, J. Biol. Chem. 263 (1988) 10408–10414.

[3] E. Pinner, E. Padan, S. Schuldiner, Cloning, sequencing, and expression of the *nhaB* gene, encoding a Na^+/H^+ antiporter in *Escherichia coli*, J. Biol. Chem. 267 (1992) 11064–11068.

[4] D.M. Ivey, A.A. Guffanti, J. Zemsky, E. Pinner, R. Karpel, E. Padan, S. Schuldiner, T.A. Krulwich, Cloning and Characterization of putative Ca^{2+}/H^+ antiporter gene from *Escherichia coli* upon functional complementation of Na^+/H^+ antiporter-deficient strains by the overexpressed gene, J. Biol. Chem. 268 (1993) 11296–11303.

[5] T. Ohyama, K. Igarashi, H. Kobayashi, Physiological role of the *chaA* gene in sodium and calcium circulations at a high pH in *Escherichia coli*, J. Bacteriol. 176 (1994) 4311–4315.

[6] E. Pinner, O. Carmel, H. Bercovier, S. Sela, E. Padan, S. Schuldiner, Cloning, sequencing and expression of the *nhaA* and *nhaR* genes from *Salmonella entiritidis*, Arch. Microbiol. 157 (1992) 323–328.

[7] T. Nakamura, Y. Komano, E. Itaya, K. Tsukamoto, T. Tsuchiya, T. Unemoto, Cloning and sequencing of an Na^+/H^+ antiporter gene from the marine bacterium *Vibrio alginolyticus*, Biochim. Biophys. Acta 1190 (1994) 465–468.

[8] T. Kuroda, T. Shimamoto, K. Inaba, M. Tsuda, T. Tsuchiya, Properties and sequence of the NhaA Na^+/H^+ antiporter of *Vibrio parahaemolyticus*, J. Biochem. 116 (1994) 1030–1038.

[9] T. Nakamura, H. Enomoto, T. Unemoto, Cloning and sequencing of the *nhaB* gene encoding an Na^+/H^+ antiporter from *Vibrio alginolyticus*, Biochim. Biophys. Acta 1275 (1996) 157–160.

[10] K. Nozaki, K. Inaba, T. Kuroda, M. Tsuda, T. Tsuchiya, Cloning and sequencing of the gene for Na^+/H^+ antiporter

of *Vibrio parahaemolyticus*, Biochem. Biophys. Res. Commun. 222 (1996) 774–779.
[11] R.D. Fleischmann, M.D. Adams, O. White, R.A. Clayton, E.F. Kirkness, A.R. Kerlavage, C.J. Bult, J.-F. Tomb, B.A. Dougherty, J.M. Merrick, K. McKenney, G. Sutton, W. FitzHugh, C.A. Fields, J.D. Gocayne, J.D. Scott, R. Shirley, L.-I. Liu, A. Glodek, J.M. Kelley, J.F. Weidman, C.A. Phillips, T. Spriggs, E. Hedblom, M.D. Cotton, T.R. Utterback, M.C. Hanna, D.T. Nguyen, D.M. Saudek, R.C. Brandon, L.D. Fine, J.L. Fritchman, J.L. Fuhrmann, N.S.M. Geoghagen, C.L. Gnehm, L.A. McDonald, K.V. Small, C.M. Fraser, H.O. Smith, J.C. Ventor, Whole-genome random sequencing and assembly of *Haemophilus influenzae* Rd., Science 269 (1995) 496–512.
[12] A. Rothman, E. Padan, S. Schuldiner, Topological analysis of NhaA, a Na^+/H^+ antiporter from *Escherichia coli*, J. Biol. Chem. 271 (1996) 32288–32292.
[13] Y. Olami, A. Rimon, Y. Gerchman, A. Rothman, E. Padan, Histidine 225, a residue of the NhaA-Na^+/H^+ antiporter of *Escherichia coli* is exposed and faces the cell exterior, J. Biol. Chem. 272 (1997) 1761–1768.
[14] T. Nakamura, Y. Komano, T. Unemoto, Three aspartic residues in membrane-spanning regions of Na^+/H^+ antiporter from *Vibrio alginolyticus* play a role in the activity of the carrier, Biochim. Biophys. Acta 1230 (1995) 170–176.
[15] H. Inoue, T. Noumi, T. Tsuchiya, H. Kanazawa, Essential aspartic acid residues, Asp-133, Asp-163 and Asp-164, in the transmembrane helices of a $Na^{+/}H^+$ antiporter (NhaA) from *Escherichia coli*, FEBS Lett. 363 (1995) 264–268.
[16] E. Pinner, E. Padan, S. Schuldiner, Kinetic properties of NhaB, a Na^+/H^+ antiporter from *Escherichia coli*, J. Biol. Chem. 269 (1994) 26274–26279.
[17] D. Taglicht, E. Padan, S. Schuldiner, Proton-sodium stoichiometry of NhaA, an electrogenic antiporter from *Escherichia coli*, J. Biol. Chem. 268 (1993) 5382–5387.
[18] E. Pinner, E. Padan, S. Schuldiner, Amiloride and harmaline are potent inhibitors of NhaB, a Na^+/H^+ antiporter from *Escherichia coli*, FEBS Lett. 365 (1995) 18–22.
[19] D.M. Engelman, T.A. Steitz, A. Goldman, Identifying nonpolar transbilayer helices in amino acid sequences of membrane proteins, Annu. Rev. Biophys. Biophys Chem. 15 (1986) 321–353.
[20] E. Brickman, J. Beckwith, Analysis of the regulation of *Escherichia coli* alkaline phosphatase synthesis using deletions and phi80 transducing phages, J. Mol. Biol. 96 (1975) 307–316.
[21] C. Manoil, J. Beckwith, TnphoA: a transposon probe for protein export signals, Proc. Natl. Acad. Sci. USA 82 (1985) 8129–8133.
[22] C. Manoil, J. Beckwith, A genetic approach to analyzing membrane protein topology, Science 233 (1986) 1403–1408.
[23] E. Bibi, O. Beja, Membrane topology of multidrug resistance protein expressed in *Escherichia coli*, N-terminal domain, J. Biol. Chem. 269 (1994) 19910–19915.
[24] E.T. Buurman, K.T. Kim, W. Epstein, Genetic evidence for two sequentially occupied K^+ binding sites in the Kdp transport ATPase, J. Biol. Chem. 270 (1995) 6678–6685.
[25] S. Danielsen, D. Boyd, J. Neuhard, Membrane topology analysis of the *Escherichia coli* cytosine permease, Microbiol. 141 (1995) 2905–2913.
[26] T. Pourcher, E. Bibi, H.R. Kaback, G. Leblanc, Membrane topology of the melibiose permease of *Escherichia coli* studied by *melB-phoA* fusion analysis, Biochem. 35 (1996) 4161–4168.
[27] D. Geller, D. Taglicht, R. Edgar, A. Tam, O. Pines, S. Michaelis, E. Bibi, Comparative topology studies in *Saccharomyces cerevisiae* and in *Escherichia coli*. The N-terminal half of the yeast ABC protein Ste6, J. Biol. Chem. 271 (1996) 13746–13753.
[28] M. van Geest, J.S. Lolkema, Membrane topology of the sodium ion-dependent citrate carrier of *Klebsiella pneumoniae*. Evidence for a new structural class of secondary transporters, J. Biol. Chem. 271 (1996) 25582–25589.
[29] D. Hanahan, Studies on transformation of *Escherichia coli* with plasmids, J. Mol. Biol. 166 (1983) 557–580.
[30] J. Sambrook, F. Fritsch, T. Maniatis, Molecular Cloning: A Laboratory Manual, 2nd edn., Cold Spring Harbor Laboratory, Cold Spring Harbor, NY, 1989.
[31] O.H. Lowry, N.J. Rosebrough, A.L. Farr, R.J. Randall, Protein measurement with the folin phenol reagent, J. Biol. Chem. 193 (1951) 265–275.
[32] J.D. Allard, K.P. Bertrand, Membrane topology of the pBR322 tetracycline resistance protein. TetA-PhoA gene fusions and implications for the mechanism of TetA membrane insertion, J. Biol. Chem. 267 (1992) 17809–17819.
[33] J. Kyte, R.F. Doolittle, A simple method for displaying the hydropathic character of a protein, J. Mol. Biol. 157 (1982) 105–132.
[34] G. von Heijne, Membrane protein structure prediction. Hydrophobicity analysis and the positive-inside rule, J. Mol. Biol. 225 (1992) 487–494.
[35] G. von Heijne, Analysis of the distribution of charged residues in the N-terminal region of signal sequences: Implications for protein export in prokaryotic and eukaryotic cells, EMBO J. 3 (1984) 2315–2318.
[36] L.Y. Jan, Y.N. Jan, Potassium channels and their evolving gates, Nature 371 (1994) 119–122.
[37] S. Stumpe, A. Schlosser, M. Schleyer, E.P. Bakker, K^+ circulation across the prokaryotic cell membrane: K^+-uptake sytems, in: W.N. Konings, H.R. Kaback, and J.S. Lolkema (Eds.), Handbook of Biological Physics. Vol. 2., Elsevier Science B.V., Amsterdam, 1996, pp. 473–500.
[38] G. von Heijne, Y. Gavel, Topogenic signals in integral membrane proteins, Eur. J. Biochem. 174 (1988) 671–678.
[39] T. Kimura, M. Suzuki, T. Sawai, A. Yamaguchi, Determination of a transmembrane segment using cysteine-scanning mutants of transposon Tn10-encoded metal–tetracycline/H + antiporter, Biochem. 35 (1996) 15896–15899.